Investigation of Whole Spine Alignment Patterns in Automotive Seated Posture Using Upright Open MRI Systems

Fusako Sato, Mamiko Odani, Yusuke Miyazaki, Taichi Nakajima,
Jacobo Antona Makoshi, Kunio Yamazaki, Koshiro Ono, Mats Svensson, Jonas Östh,
Shigehiro Morikawa, Sylvia Schick, Antonio Ferreiro Perez

Abstract The purpose of this study is to investigate whole spinal alignment patterns in an automotive seated posture. Image data sets of eight female and seven male seated volunteers were acquired using upright open Magnetic Resonance Imaging systems. The images were processed to extract the whole spine alignment defined with the centres of the vertebral bodies. Patterns of the whole spine alignment were investigated through Multi-Dimensional Scaling analyses. The analysis revealed that variations in the whole spine alignment due to individual differences were seen most remarkably in the combination of curvature of the cervical spinal alignment and degree of the thoracic kyphosis with its peak vertebra level. Subjects with cervical lordosis tended to have a pronounced thoracic kyphosis, with the peak of this kyphosis located at a lower vertebra level. Subjects with cervical kyphosis tended to have a less pronounced thoracic kyphosis, with the peak of this kyphosis at a higher vertebra level. These trends were also observed in the differences of average spinal alignments between males and females.

Keywords Driving posture, Spinal alignment, MRI, Multi-Dimensional Scaling, Automotive.

I. INTRODUCTION

Several types of whiplash protection seat have been installed since the late 1990s [1-4]. Analysing insurance claim records, a number of whiplash protection seats have reduced the risk of sustaining whiplash associated disorders (WAD) more effectively for males than for females [5-6]. In order to provide more effective preventive measures against WAD for females as well as males, further investigations into the injury biomechanics of WAD are needed.

Previous experimental studies with post-mortem human head-neck samples have reported that the initial cervical curvature affected the neck injury severity [7-12]. In a series of finite element (FE) analyses [13], a head-neck FE model with kyphotic cervical alignment exhibited larger elongations of the facet joint ligaments than one with lordotic cervical alignment in rear impact conditions. As reported by Matsumoto *et al*. [14], females are more likely than males to have non-lordotic cervical alignment.

Rear impact sled tests with human volunteers [15] showed influences of the interaction between the dorsal region and seatback on the cervical kinematics and its importance when understanding the injury mechanisms of WAD in rear impact conditions. Rear impact reconstruction simulations with a whole body human FE model have also demonstrated that the initial position of the thoracolumbar spine as well as that of cervical spine affects the cervical vertebral kinematics [16].

Despite being one of the key factors for further investigation of WAD, as shown by these previous studies, the alignment of the whole spine, from cervical spine to the sacrum, in an automotive seated posture has not been well reported, particularly not for females [17]. Our previous study [18] illustrated intervertebral angles from C2 through the sacrum showed different trends between seated and supine postures, even thoracic region. Following the previous study, the spinal alignment in a seated posture was focused in this study. The purpose of

F. Sato is a researcher (e-mail: fsatou@jari.or.jp; tel: +81-29-856-0885), T. Nakajima and J. Antona Makoshi are researchers, K. Yamazaki is a manager in the Department of Crash Safety Research and K. Ono is the Executive Research Adviser & Research Director, all at Japan Automobile Research Institute (JARI). M. Odani is a MSc student and Y. Miyazaki is an associate professor at the Tokyo Institute of Technology, Japan. F. Sato is a PhD student, J. Östh is a Researcher and M.Y. Svensson is a Professor at Chalmers University of Technology, Sweden. S. Morikawa is a medical doctor and Professor in Shiga University of Medical Science, Japan. S. Schick is a medical doctor and researcher in Ludwig-Maximilians-Universitaet Muenchen Institute of Legal Medicine, Germany. A. Ferreiro Perez is a medical doctor and Professor in Fundación de Investigación HM Hospitales.

this study is to obtain the geometry of the spinal column in an automotive seated posture, using an upright open magnetic resonance imaging (MRI) system, and to investigate and provide the whole spinal alignment patterns by Multi-Dimensional Scaling (MDS). Multi-Dimensional Scaling is a method to illustrate similarities of objects, and is used here to analyse representative spinal alignment patterns.

II. METHODS

Image data of subjects in a seated posture were acquired by an upright open MRI system that could take a scan without the risk of ionising radiation. The MRI systems used were located at Shiga University of Medical Science, Japan, and Hospital Universitario HM Montepríncipe (Fundación de Investigación HM Hospitales), Spain. The spinal alignment of each subject was extracted from the MRI data, and patterns of spinal alignments were investigated via the MDS method. All procedures in this study were approved by the Institutional Review Board of Shiga University of Medical Science and by Hospital Universitario HM Montepríncipe and the Japan Automobile Research Institute, and adhered to the guidelines of all ethical committees.

Human Subjects

Eight female and seven male healthy adult volunteers were recruited, ranging in age from 21 to 38 years with an average age of 27 years, and with characteristic data according to Tables I and II. All subjects had no known spinal disease and no contraindications for MRI, including claustrophobia, metal implants and implanted electrical devices. The subjects consisted of five Japanese and three European females, and three Japanese and four European males. Japanese subjects were selected based on the average Japanese body size (height and weight) in their age from 20 to 40 years: 159 ± 5 cm and 51 ± 6 kg for females; 172 ± 6 cm and 67 ± 9 kg for males [mean ± standard deviation (SD)] [19]. European subjects were selected based on the body size of the the dummy family defined in the University of Michigan Transportation Research Institute (UMTRI) study [20]: mid-sized female of 161.8 cm and 62.3 kg; and mid-sized male of 175.3 cm and 77.3 kg.

TABLE I
CHARACTERISTICS OF THE JAPANESE SUBJECTS

Subject ID	Sex	Height [cm]	Weight [kg]	Age [y]
F-J-1	Female	158	47	22
F-J-2	Female	158	44	23
F-J-3	Female	156	41	22
F-J-4	Female	157	54	35
F-J-5	Female	169	55	21
M-J-1	Male	171	68	24
M-J-2	Male	172	61	23
M-J-3	Male	162	49	23

TABLE II
CHARACTERISTICS OF THE EUROPEAN SUBJECTS

Subject ID	Sex	Height [cm]	Weight [kg]	Age [y]
F-E-1	Female	164	57	32
F-E-2	Female	165	57	29
F-E-3	Female	157	61	33
M-E-1	Male	176	78	34
M-E-2	Male	175	79	24
M-E-3	Male	175	83	38
M-E-4	Male	175	72	32

Image acquisition

The spinal column was scanned in a seated posture with an upright open MRI system, Signa SP/i (0.5T, the horizontal gap of the magnets: 60 cm, GE Healthcare Inc.) at Shiga University of Medical Science for Japanese subjects, and with a Fonar Upright Multi-Position MRI system (0.6T, the horizontal gap of the magnets: 46 cm, Fonar Inc.) at Hospital Universitario HM Montepríncipe for the European subjects, respectively (Fig. 1). The main acquisitions were carried out with T1-weighted 3D gradient echo sequence in a sagittal plane. A wooden seat was placed in a MRI system, and subjects were seated. The seat consisted of two rigid planes with a seatback inclined by 20 degrees from the vertical level and a seat pan inclined by 10 degrees from the horizontal level. The seat was designed to correspond to a laboratory seat utilised for a series of rear impact sled tests in a previous volunteer study [21]. The seated positioning of subjects was carried out with the procedure as the previous volunteer sled tests [21]. Subjects were seated as deeply as possible on the wooden seat in a relaxed state, and asked to face forward with the Frankfort plane 10 degrees upward from the horizontal. The femurs (the line between the great trochanter and the centre of the knee joint) were set at 25 degrees upward from the horizontal. To capture the full spinal column from the bottom of the skull to the sacrum, three or four image acquisitions were made with enough overlap to cut off geometric warping of MRI

images at the edge of the filed (Fig. 2). The position of the seat was adjusted to fit the field of view for the MRI machine. All the image data were acquired in less than 2.5 hours including seat adjustment for each subject. Then, image data were combined manually for each subject.

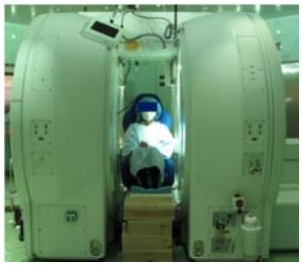

(a) Shiga University of Medical Science.

(b) Hospital Universitario HM Montepríncipe.

Fig. 1. Seated posture in the upright open MRI system.

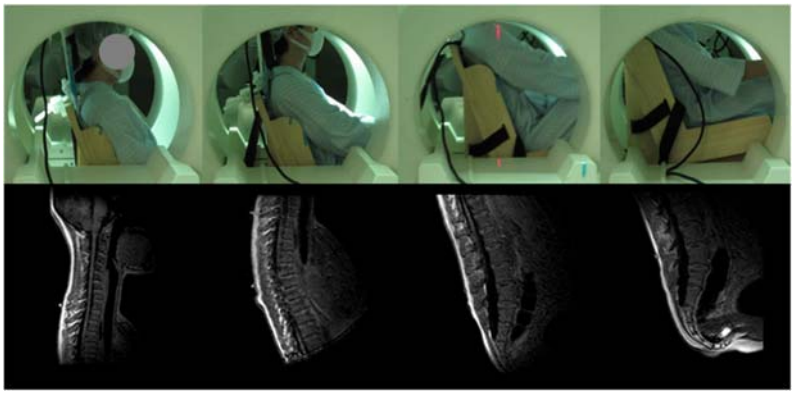

(a) Neck. (b) Chest. (c) Abdomen. (d) Pelvis.

Fig. 2. MRI scanning in seated posture

Image data-processing

The spinal alignments defined with the centres of the vertebral bodies (Fig. 3) were extracted from midsagittal images by the medical imaging software OsiriX (Pixmeo, Geneva, Switzerland). In the spinal alignment definition, the location of C2 was set on the the midpoint of the inferior surface of the C2 vertebral body. For the sacrum, the midpoint of the superior surface was used. Thereafter, rotation and normalisation processing of the spinal alignment was conducted to set C2 at 1 on the normalised z-axis, with sacrum at the origin, as shown in Fig. 4(a). For analyses of the cervical, thoracic and lumbar spine, rotation and normalisation processing was also conducted, as shown in Fig. 4 (b)–(d).

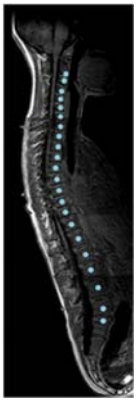

Fig. 3. Spinal alignment in midsagittal image data.

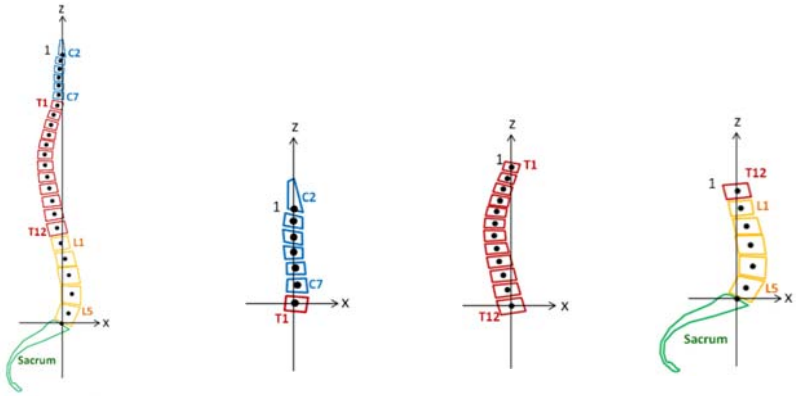

(a) Whole spine. (b) Cervical spine. (c) Thoracic spine. (d) Lumbar spine

Fig. 4. Spinal alignments in the normalised coordinate system.

Distribution of spinal alignments by MDS

In order to investigate spinal alignment patterns in the seated posture, spinal alignments were analysed using MDS. Multi-Dimensional Scaling is a multivariate analysis technique used to provide a scatterplot that displays the relative positions of objects with data dimensions reduced as much as possible, while retaining the original pairwise distances between the objects as much as possible. MDS detects meaningful underlying dimensions in a data set, so that similar object are plotted closely and dissimilar objects are plotted further apart in a scatterplot. Hence, anatomical characteristics can be classified when conducting a MDS analysis on a set of anatomical shape data [22-23]. The input data for MDS is in the form of a distance matrix *D*, representing the Euclidean pairwise distances between objects in Equation (1):

$$D = \begin{pmatrix} e_{11} & \cdots & e_{1n} \\ \vdots & \ddots & \vdots \\ e_{n1} & \cdots & e_{nn} \end{pmatrix} \quad (1)$$

where, *n* means *n*-th object. In the current study, the distance matrix *D* was represented by the inter-individual distances between all possible pairs of subjects. An inter-individual distance between two subjects e_{st} (Fig. 5) was expressed in the sum of squares of Euclidean pairwise distances between corresponding vertebrae s_i and t_i in Equation (2):

$$e_{st} = \sum_{i=1}^{j} (s_i - t_i)^2 \quad (2)$$

where, s_i and t_i contain x and z coordinate values of a corresponding vertebra for subjects *S* and *T* in the normalised coordinate system, and *j* is the total number of the vertebral points shown in Fig. 4. In a MDS analysis on the distance matrix *D*, MDS dimensions are represented by eigenvectors of *D* in descending order of eigenvalues, which explain the amount of variance in each direction. For example, the 1st MDS dimension is defined with an eigenvector corresponding to the largest eigenvalue, and points in the direction of maximum variance in the data. This means that the 1st MDS dimension can portray the distance relations between subjects most efficiently [22-23].

One of the aims to carry out an MDS analysis is to obtain a fairly good approximate representation of a data set in a scatterplot with a small number of dimensions. The reduction in dimensionality was achieved based on the contribution ratio and the cumulative contribution ratio of each MDS dimension. The contributions ratio of the *k*-th MDS dimension is given by the ratio of the *k*-th eigenvalue to the sum of all eigenvalues, and the cumulative contribution ratio by the sum of the first *k* contribution ratios. Thereafter, a distribution map of spinal alignments was created, with MDS scores of each subject in the reduced MDS dimensions. MDS scores are obtained by *vD*, where v is a matrix of eigenvectors of *D*. Since the MDS dimensions express independent shape factors [22-23], spinal alignment patterns were investigated by interpreting the underlying meanings of the MDS dimensions based on the MDS scores of each subject on the distribution map. Interpretation of the MDS dimensions effects on the spinal alignment is explained in anatomical terms in Section III: Results.

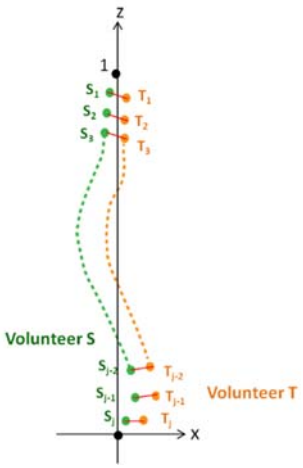

Fig. 5. Inter-individual distance between two subjects.

Estimation of representative spinal alignment patterns

On the distribution map of whole spine alignments, the representative alignment patterns on the 50% probability ellipsoid and the average spinal alignment patterns for female, male and all subjectswere estimated by weighted average of whole spinal alignments, expressed in Equation (3) below. By interpreting underlying shape factor of each MDS dimension through the representative and average spinal alignments, patterns of spinal alignments can be investigated. In order to obtain the MDS score of the estimated average spinal alignment, an MDS analysis, including the estimated spinal alignments, was carried out. Thereafter, the weight factor, c_j in Equation (3), was calculated so as to minimise the difference between the MDS score of the estimated spinal alignment and the target MDS score. The target MDS scores are the intersections of the 50% probability ellipsoid and the axes of the 1st or 2nd MDS dimensions, the average MDS scores for females and males, and the origin of the distribution map. The origin represents the average for all subjects. Per Equation (3):

$$A_{ave} = \sum_{j=1}^{N} c_j A_j \tag{3}$$

where, A_{ave} is the weighted average of spinal alignments, A_j is the spinal alignment of j-th subject in Equation (4) below and N is the number of subjects.

$$A_j = \begin{pmatrix} x_{j1} & z_{j1} \\ \vdots & \vdots \\ x_{j22} & z_{j22} \end{pmatrix} \tag{4}$$

III. RESULTS

Patterns of the spinal alignments in the seated posture were analysed using midsagittal images acquired by an upright open MRI system. Figure 6 shows examples of the midsagittal images for female and male subjects, respectively. The normalized whole spine alignments at their original positions are provided in Appendix. From the MDS analyses on spinal alignments extracted from the image data, individual variability with the maximum variance was seen in a spinal characteristic consisting of curvature of the cervical spinal alignment and degree of the thoracic kyphosis with its peak vertebra level through interpretations of the MDS dimensions, as outlined in the following sections.

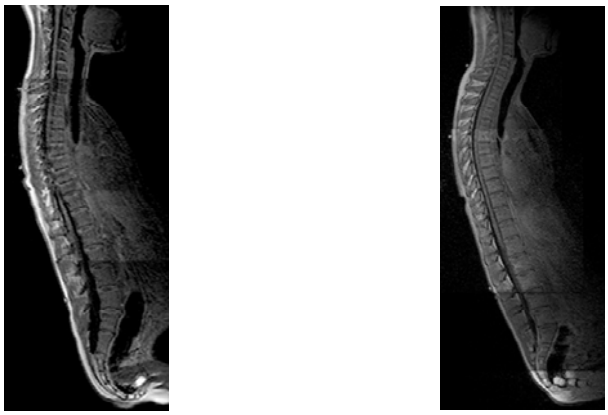

(a) Female. (b) Male.

Fig. 6. Midsagittal images of the seated posture.

Distribution of spinal alignments by MDS

The distribution map of whole spine alignments is shown in Fig. 7. The contribution ratio is 67% for the 1st MDS dimension, 20% for the 2nd MDS dimension, 9% for the 3rd MDS dimension, 3% for the 4th MDS dimension and so on. The current study selected up to the 2nd MDS dimensions in order to simplify the investigation of patterns in spinal alignments. The distribution map was created with the 1st and 2nd MDS dimensions, as shown in Fig. 7. The distribution map explained 87% of total variance of whole spine alignments. With comparison between subjects varied on the 1st MDS dimension with similar MDS scores on the 2nd MDS dimension, subjects identified as number 1 and 2 (shown in Fig. 7(b)) for example, the 1st MDS dimension was interpreted as a shape factor of the whole spine alignment. Subjects in the positive region of the 1st MDS dimension had lordotic cervical and more pronounced kyphotic thoracic spine, with a peak of the thoracic kyphosis (the most backward vertebra of the thoracic spine) at a lower vertebra level. Subjects in the negative region of the 1st MDS dimension had kyphotic cervical and less-kyphotic thoracic spine with a peak of the thoracic kyphosis at a higher vertebra level. Therefore, the 1st MDS dimension seems to indicate the combination of curvature of the cervical spinal alignment and degree of the thoracic kyphosis, with its peak vertebra level as a shape factor to explain variation in the whole spine alignment most efficiently. Likewise, in order to interpret the 2nd MDS dimension, the spinal alignment was compared between subjects identified as number 3 and 4 in Fig. 7(c). Subjects in the positive region of the 2nd MDS dimension had thoracolumbar spine more forward than subjects in the negative region of the 2nd MDS dimension. Hence, the 2nd MDS dimension seems to indicate the position of thoracolumbar region as a second shape factor for the whole spine alignment. Most females (one of eight female subjects) have negative score on the 1st MDS dimension. Subjects with positive score on the 1st MDS dimension were mostly males (four males of five subjects).

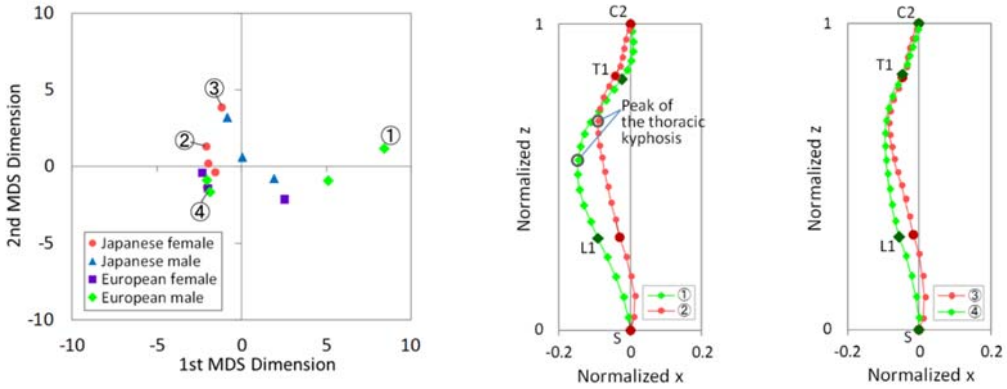

(a) Two-dimensional distribution map for whole spine alignments. (b) Comparison on the 1st MDS dimension. (c) Comparison on the 2nd MDS dimension.

Fig. 7. MDS analysis on whole spine alignments. Numbers shown in Fig. 7(a) correspond to IDs for spinal alignments in Fig. 7(b) and (c).

The distribution map of cervical spinal alignments from C2 to T1 consists of the first two MDS dimensions as with the distribution map of whole spine alignments (Fig. 8). The contribution ratio is 78% for the 1st MDS dimension and 22% for the 2nd MDS dimension. With comparison of the cervical spinal alignment between Subject 1 and 3, for example (shown in Fig. 8(b)), the cervical spinal alignments with positive MDS score on the 1st MDS dimension tend to lordosis, while those with negative MDS score tend to have kyphosis. Hence, the 1st MDS dimension indicates curvature types of the cervical spinal alignment. For the 2nd MDS dimension, noticeable characteristics were not found out. Similar to the whole spine alignment, most females have a negative score on the 1st MDS dimension. Subjects with positive score on the 1st MDS dimension were mostly males.

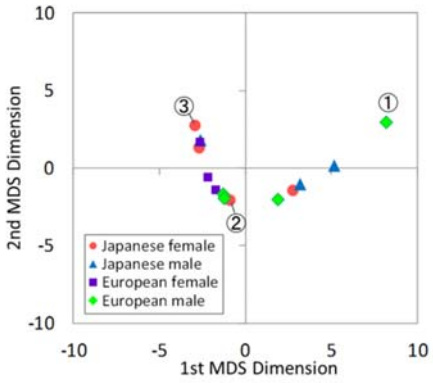

(a) Two-dimensional distribution map for cervical spinal alignments.

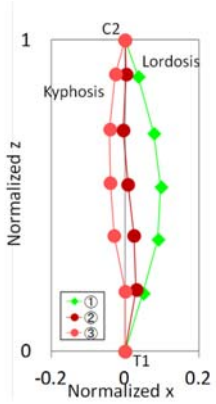

(b) Comparison on the 1st MDS dimension.

Fig. 8. MDS analysis on cervical spinal alignments. Numbers shown in Fig. 8(a) correspond to IDs for cervical spinal alignments in Fig. 8(b).

For the thoracic spinal alignments from T1 to T12 (Fig. 9(a)), the contribution ratio is 69% for the 1st MDS dimension and 21% for the 2nd MDS dimension. Figure 9(b) shows an example for comparisons of the thoracic spinal alignment to investigate the meaning of the 1st MDS dimension. The peak of the thoracic kyphosis is more backward at a lower vertebra level for subjects in the positive region of the 1st MDS dimension than those in the negative region. The 1st MDS dimension indicates the position of a peak of the thoracic kyphosis and peak vertebra level. For the 2nd MDS dimension, Fig. 9(c) explains that it indicates degree of the thoracic kyphosis with similar thoracic spinal alignments.

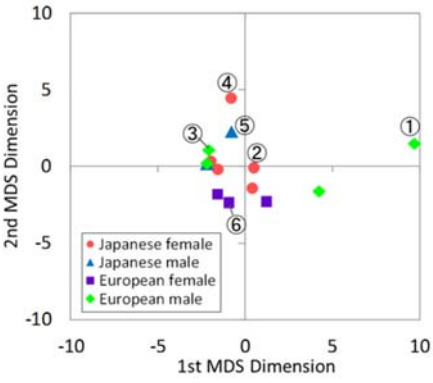

(a) Two-dimensional distribution map for thoracic spinal alignments.

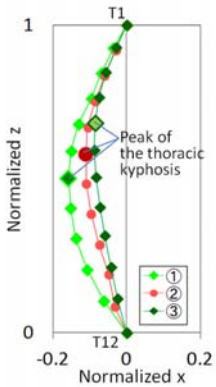

(b) Comparison on the 1st MDS dimension.

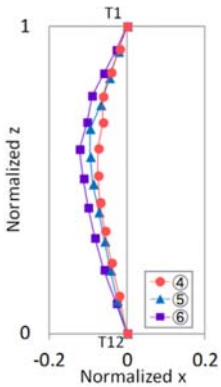

(c) Comparison on the 2nd MDS dimension.

Fig. 9. MDS analysis on thoracic spinal alignments. Numbers shown in Fig. 9(a) correspond to IDs for thoracic spinal alignments in Fig. 9(b) and (c).

In the two-dimensional distribution map of lumbar spinal alignments from T12 to the sacrum (Fig. 10(a)), the contribution ratio is 53% for the 1st MDS dimension and 40% for the 2nd MDS dimension. In Fig. 10(b), the lumbar lordosis is more pronounced, with an increase in MDS score of the 1st MDS dimension. The 1st MDS dimension indicates degree of the lumbar lordosis. For the 2nd MDS dimension, noticeable characteristics were not found out.

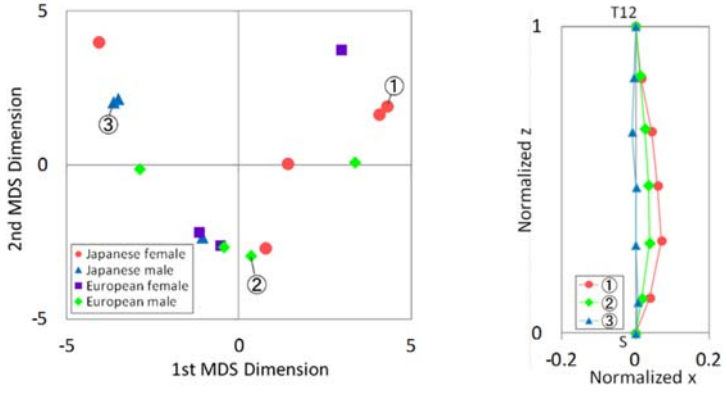

(a) Two-dimensional distribution map for lumbar spinal alignments.

(b) Comparison on the 1st MDS dimension.

Fig. 10. MDS analysis on lumbar spinal alignments. Numbers shown in Fig. 10(a) correspond to IDs for lumbar spinal alignments in Fig. 10(b).

The correlations between the MDS dimensions are shown in Fig. 11. The 1st MDS dimensions of the cervical spinal alignment and the thoracic spinal alignment correlate positively with the 1st MDS dimension of the whole spine alignment, respectively. There were no correlations seen in other pairs of the MDS dimensions.

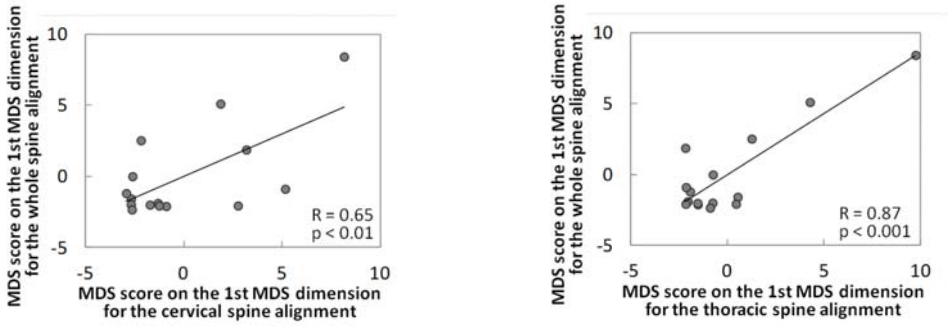

(a) (b)

Fig. 11. Correlations of the 1st MDS dimension between the whole spine alignment and the cervical or thoracic spinal alignment. R is the correlation coefficient and p is p-values from t-test.

Estimation of representative spinal alignment patterns

The representative whole spine alignment patterns estimated on the 50% probability ellipsoid are shown with the two-dimensional distribution map, including those representative alignments in Fig. 12. A Kolmogorov-Smimov normality test was carried out to assess the normality of the data, and it was found that the 2nd MDS dimension showed $p < 0.05$ while the 1st MDS dimension indicated $p > 0.05$ due to the limited number of subjects. The MDS scores for the representative alignment patterns were slightly off the intersections of the 50% probability ellipsoid and the axes of the 1st or 2nd MDS dimensions due to the limited number of subjects also. When comparing the estimated spinal alignment patterns at the intersections of the 50% probability ellipsoid and the axes of the 1st MDS dimension – the estimated alignment 1 and 2 in Fig. 12(b) – the estimated spinal alignment pattern in the positive region of the 1st MDS dimension is a lordotic cervical

and a more pronounced kyphotic thoracic spine, with a peak of the thoracic kyphosis at a lower vertebra level. On the other hand, the estimated spinal alignment pattern in the negative region of the 1st MDS dimension is a kyphotic, or almost straight, cervical and a less-kyphotic thoracic spine, with a peak of the thoracic kyphosis at a higher vertebra level. For the estimated patterns at the intersections of the 50% probability ellipsoid and the axes of the 2nd MDS dimension – the estimated alignment 3 and 4 in Fig. 12(c) – the thoracic spine is more forward for the estimated spinal alignment pattern in the positive region of the 2nd dimension than that in the negative region of the 2nd MDS dimension.

The estimated average spinal alignment patterns for both genders are shown with the two-dimensional distribution map, including those two alignments in Fig. 13. The average MDS score of females was negative, while that of males was positive on the 1st MDS dimension (p-values from t-test: p<0.1) with the MDS score of the 2nd MDS dimension close to zero. The estimated average spinal alignment pattern of females was slightly kyphotic, or almost straight, cervical and less-kyphotic thoracic spine, while that of males was lordotic cervical and more pronounced kyphotic thoracic spine.

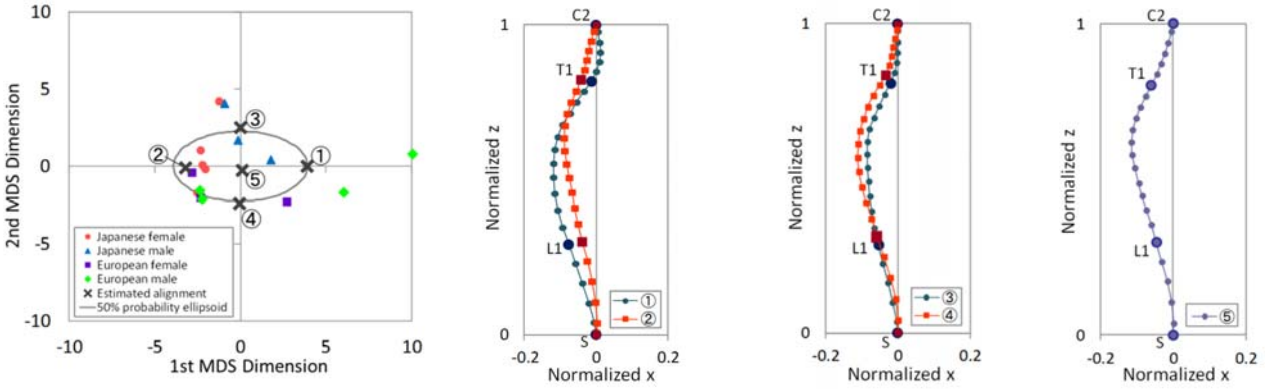

(a) Two-dimensional distribution map for whole spine alignments with the 50% probability ellipsoid.

(b) Estimated whole spine alignment patterns at the intersections of the 50% probability ellipsoid and the axes of the 1st MDS dimension.

(c) Estimated whole spine alignment patterns at the intersections of the 50% probability ellipsoid and the axes of the 2nd MDS dimension.

(d) Estimated whole spine alignment pattern at the origin of the distribution map.

Fig. 12. Representative whole spine alignment patterns estimated on the 50% probability ellipsoid. Numbers shown in Fig. 12(a) correspond to IDs for spinal alignments in Fig. 12(b), (c) and (d). The origin of the distribution map (Fig. 12(a)) means the average MDS score of all subjects. The estimated whole spine alignment pattern at the origin of the distribution map indicates the average for all subjects.

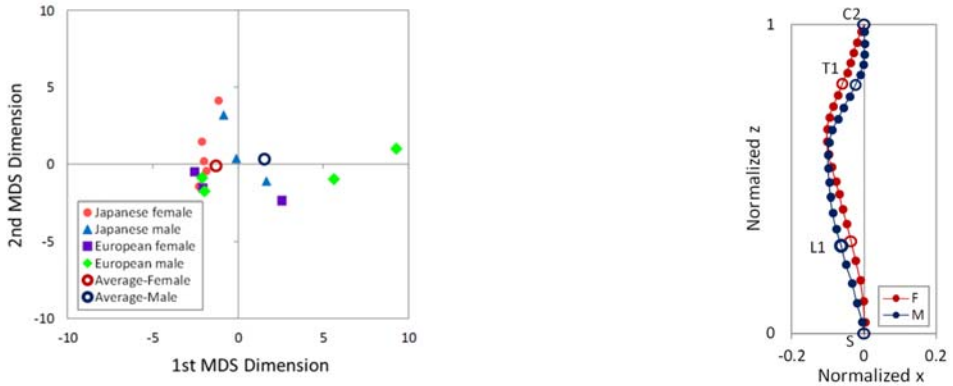

(a) Two-dimensional distribution map for whole spine alignment with average MDS scores for female and male subjects.

(b) Estimated average spinal alignment for both genders. “F” indicates the estimated spinal alignment at the average MDS score for females in the distribution map. “M” indicates the estimated average spinal alignment at the average MDS score for males.

Fig. 13. Estimated average spinal alignment patterns for both genders.

IV. DISCUSSION

In the current study, upright open MRI systems were used to capture the spinal alignment in a seated posture. Then, patterns of spinal alignments in a seated posture were investigated by MDS analyses. MDS has a similar mathematical process to Principal Component Analysis (PCA). MDS portrays similarities of subjects in near distances on a lower dimensional space by using a distance matrix, while PCA finds out the directions of maximum variability by using the data set itself, instead of pairwise distances of subjects [24-25]. In order to investigate patterns of the spinal alignment from the point of view of the similarities of spinal alignments, MDS was chosen in this study.

In the MDS analysis, The 1st MDS dimension of the whole spine alignment (Fig. 7) indicated that the whole spine alignment tends to shift from the combination of kyphotic cervical and less-kyphotic thoracic spine, with a peak of the thoracic kyphosis at a higher vertebra level to lordotic cervical, and more pronounced kyphotic thoracic spine with a peak of the thoracic kyphosis at a lower vertebra level in accordance with the increase of MDS score on the 1st MDS dimension. Likewise, representative spinal alignment patterns estimated on the intersection points of the 50% probability ellipsoid and the axis of the 1st MDS dimension on the distribution map in Fig. 12 corresponded to such a trend. In addition, the 1st MDS dimension of the whole spine alignment had positive correlations with the 1st MDS dimensions of the cervical spinal alignment and the thoracic spinal alignment, as shown in Fig. 11. On the 1st MDS dimension of the cervical spinal alignment, the cervical spinal alignment tends to shift from kyphosis to lordosis with the increase of the MDS score (Fig. 8). The 1st MDS dimension of the thoracic spinal alignment indicated that the peak of the thoracic kyphosis tend to be more backward at a lower vertebra level with greater MDS score. Those results also supported the observation on the distribution map of whole spine alignments. Spinal categories, for instance male spines, which are found to have a more pronounced curvature in one spinal region tend to have more pronounced curvatures in their other spinal regions. Therefore, variations in the whole spine alignment due to individual differences seems to appear most remarkably in the combination of curvature of the cervical spinal alignment and degree of the thoracic kyphosis with its peak vertebra level. Indeed, the difference of the estimated average spinal alignments between genders corresponded to those results (Fig. 13(b)). For the 2nd MDS dimension of the whole spine alignment (Fig. 7), the thoracolumbar region tend to be more forward in accordance with the increase of MDS score on the 2nd MDS dimension. Likewise, representative spinal alignment patterns estimated on the intersection points of the 50% probability ellipsoid and the axis of the 2nd MDS dimension on the distribution map in Fig. 12 showed such trend in the thoracic region. Hence, forward/backward position of the thoracolumbar region seems to be a second shape factor to explain variation in the whole spinal alignment.

As reported in previous studies on the variation in the cervical spinal alignment [14][26-27], gender is an independent factor and has a significant correlation with non-lordosis. Females are more likely than males to present non-lordosis (kyphotic or straight). Conversely, males present more pronounced lordosis statistically [14][26-27]. In the current study, the results indicated that the cervical region of the estimated average spinal alignment was non-lordotic for females and lordotic for males (Fig. 13(b)), in agreement with the previous studies. Klinich *et al.* [28-29] also analysed the cervical spine curvature in an automotive seated posture with 180 subjects including both genders. The study illustrated approximately three-quarters of subject had a slightly lordotic and relatively straight curvature in appearance. The estimated average spinal alignment for all subject in Fig. 12(d) have a slightly lordotic cervical curvature, and corresponds to the result in the previous papers. Furthermore, when comparing the spinal alignment between seated and supine postures, our previous study [18] showed the spinal alignment was influenced by the orientation of gravity, even in thoracic spine. Newell *et al.* [30] also demonstrated an effect of gravity on the cervical spinal alignment by comparing between seated upright and inversed. Therefore, it was essential to set a seated posture under appropriate orientation of gravity in order to investigate the spinal alignment in a seated posture in this study.

At the cervicothoracic junction, a relationship between T1 inclination and the cervical spinal alignment was reported in previous studies [31-32]. T1 inclination was more forward for males than females. The cervical spinal alignment tended to be more hypo-lordosis or kyphosis with decreasing T1 inclination. In this study, the estimated average spinal alignment for females has a less forward inclination around T1 with less-lordotic cervical spine than that for males. The trend observed in this study was consistent with the previous studies.

Regarding the lumbar region, the lumbar lordosis, which is defined as the relative angle between L1 and the sacrum, was significantly greater for females than males in an upright seated position, as reported in [33]. The average spinal alignments for both genders estimated in this study with an automotive seated posture indicated that the lumbar spinal alignment was a slightly more pronounced lordosis for females than males (Fig. 13).

The seat used in this study was a laboratory seat consisting of just two flat panels, therefore it may not cause the sitting height to be a factor that could explain individual differences in the spinal alignment due to the flatness of the seating surface. This means differences in the spinal alignment can be more easily tracked to gender, and would result in such gender differences as were observed in this study. Further investigation would be needed to access the spinal alignment patterns with commercially available automotive seat. Seat properties (foam and frame stiffness and so on) and seat positioning (seat back angle, steering wheel placement and so on) might affect the spinal alignment.

This study focused on the spinal alignment and extracted it from the MRI data. The MRI data also contains spinal cord, flesh, hart, diaphragm, stomach and so on. As a next step, future research will address to investigate spinal alignment three-dimensionally and its relationship with organs and soft tissues (size, shapes and positions) using the MRI data.

Limitations

The image data used in this study was acquired from eight females and seven males. It was insufficient to classify spinal alignment patterns in more detail and to generalise characteristics of the spinal alignment in a specific group of subjects, even in ages, since all subjects were in the 20–40 age group. In addition, subjects participating in this study were from Japan and European countries. Although cultural differences in everyday activity might affect their skeletal structures, this study have not taken such differences into account. Furthermore, data was acquired with two different MRI systems at two locations, which potentially might have an effect on the results. We are however confident that this effect was small since we had enough overlap between images so that no distortion effects at the edge of the imaging field influenced the result. Results obtained in the current study will enable researchers to determine the whole spine alignment more accurately in the definition of initial posture for human body FE models and to conduct improved computer simulations of vertebral kinematics for further investigation into injury mechanisms of WAD.

V. CONCLUSIONS

This study investigated patterns of the whole spine alignment in a seated posture by using an upright open MRI system that could take a scan without the risk of ionising radiation. Through MDS analyses on spinal alignments, variations in the whole spine alignment due to individual differences were seen most remarkably in the combination of curvature of the cervical spinal alignment and degree of the thoracic kyphosis with its peak vertebra level. Subjects with a lordotic cervical spinal alignment tend to have a more pronounced kyphotic thoracic spine, with a peak of the thoracic kyphosis at a lower vertebra level. Subjects with a kyphotic cervical spinal alignment tend to have a less-kyphotic thoracic spine, with a peak of the thoracic kyphosis at a higher vertebra level. Those trends were also observed in the differences of the estimated average spinal alignments between genders.

VI. ACKNOWLEDGEMENTS

This work was supported by JSPS KAKENHI Grant Number 15K17945. For their assistance with this study the authors thank: Masahiro Yoshimura and Harumi Iguchi from the Department of Radiology at Shiga University of Medical Science, Japan; Dr Makiko Kouchi and Yuko Kawai from Digital Human Research Centre at National Institute of Advanced Industrial Science and Technology, Japan; Javier Montero from Hospital Universitario HM Montepríncipe, Spain; and Beatriz Nácher Fernández and her colleagues from Instituto de Biomecánica de Valencia, Spain.

VII. REFERENCES

[1] Wiklund, K., Larsson, H. SAAB Active Head Restraint (SAHR) – Seat Design to Reduce the Risk of Neck Injuries in Rear Impacts. SAE paper no. 980297, 1997.

[2] Lundell, B., Jakobson, L., Alfredsson, B., Lindstrom, M., Simonsson, L. The WHIPS Seat – A Car Seat for Improved Protection Against Neck Injuries in Rear End Impacts. *Proceedings of 16th ESV Conference,* 1998, Windsor (Canada), Paper No. 98-S7-O-08, 1586-1596.

[3] Jakobsson, L. (1997) Automobile Design and Whiplash Prevention, pp.299–306. In Robert Gunzberg & Maerk Szpalski, Whiplash Injuries: Current Concepts in Prevention, Diagnoses and Treatment of the Cervical Whiplash Syndrome. *Lippincott-Raven Publishers*, Philadelphia, USA.

[4] Sekizuka, M. Seat Designs for Whiplash Injury Lessening. *Proceedings of 16th ESV Conference,* 1998, Windsor (Canada), Paper No. 98-S7-O-06, 1570-1578.

[5] Kullgren, A., Krafft, M. Gender analysis on whiplash seat effectiveness: results from real-world crashes. *Proceedings of IRCOBI Conference,* 2010, Hannover (Germany).

[6] Kullgren, A., Stigson, H., Krafft, M. Development of whiplash associated disorders for male and female car occupants in cars launched since the 80s in different impact directions. *Proceedings of IRCOBI Conference,* 2013, Göteborg (Sweden).

[7] Maiman, D. J., Sances A. Jr. *et al*. (1983) Compression injury of the cervical spine. *Neurosurgery*, **13**(3): pp.254–60.

[8] Maiman, D. J., Yoganandan, N., Pintar, F. A. (2002) Preinjury cervical alignment affecting spinal trauma. *J Neurosurgery*, **97**: pp.57–62.

[9] Yoganandan, N., Sances, A. Jr. *et al*. (1986) Experimental spinal injuries with vertical impact. *Spine*, **11**(9): pp.855–60.

[10] Yoganandan, N., Pinter, F. A., Gennarelli, T. A., Eppinger, R. H., Voo, L. M. Geometrical effects on the mechanism of cervical spine injury due to head impact. *Proceedings of IRCOBI Conference*, 1999, Sitges (Spain).

[11] Liu, Y. K., Dai, Q. G. (1989) The second stiffest axis of a beam-column: implications for cervical spine trauma. *J Biomech Eng*, **111**(2): pp.122–7.

[12] Pinter, F., Yoganandan, N. *et al*. Dynamic Characteristics of the Human Cervical Spine. *Proceedings of 39th Stapp Car Crash Conference*, 1995, San Diego, Ca.

[13] Stemper, B. D., Yoganandan, N., Pinter, F. A. (2005) Effects of abnormal posture on capsular ligament elongations in a computational model subjected to whiplash loading. *J Biomech*, **38**(6): pp.1313–23.

[14] Matsumoto, M., Fujimura, Y., Suzuki, N., Toyama, Y., Shiga, H. (1998) Cervical curvature in acute whiplash injures: prospective comparative study with asymptomatic subjects. *Injury*, **29**(10): pp.775–8.

[15] Ono, K., Inami, S. *et al*. Relationship between localized spine deformation and cervical vertebral motions for low speed rear impacts using human volunteers. *Proceedings of IRCOBI Conference*, 1999, Barcelona (Spain).

[16] Sato, F., Antona, J., Ejima, S., Ono, K. Influence on cervical vertebral motion of the interaction between occupant and head restraint/seat, based on the reconstruction of rear-end collision using finite element human model. *Proceedings of IRCOBI Conference*, 2010, Hannover (Germany).

[17] Chabert, L., Ghannouchi, S., Cavallero, C. Geometrical characterisation of a seated occupant. *Proceedings of 16th ESV Conference*, 1998, Ontario (Canada).

[18] Sato, F., Odani, M. *et al*., (2016) Analysis of the alignment of whole spine in automotive seated and supine posture using an upright open MRI system. International Journal of Automotive Engineering, **7**(1): pp. 29-35.

[19] Ministry of Education, Culture, Sports, Science and Technology, Japan. (2012) Annual Report of Anthropometry data by age in 2012, http://www.e-stat.go.jp/SG1/estat/List.do?bid=000001050841&cycode=0, (accessed: 1 February 2015).

[20] Schneider, L. W., Robbins, D. H., Pflug, M. A., Snyder, R. G. (1983) Development of Anthropometrically Based Design Specifications for an Advanced Adult Anthropomorphic Dummy Family. *University of Michigan Transportation Research Institute*, Final Report, UMTRI-83-53-1.

[21] Ono, K., Ejima, S. *et al*. Prediction of neck injury risk based on the analysis of localized cervical vertebral motion of human volunteers during low-speed rear impacts. *Proceedings of IRCOBI Conference,* 2006, Madrid, Spain.

[22] Miyazaki, Y., Ujihashi, S., Mochimaru, M., Kouchi, M. Influence of the head shape variation on brain damage under impact. *Proceedings of SAE Digital Human Modeling for Design and Engineering symposium*, 2005, Iowa City, USA.
[23] Mochimaru, M., Kouchi, M. Statistics for 3D human body forms. *Proceedings of SAE Digital Human Modeling for Design and Engineering Conference and Exposition*, 2000, Dearborn (Michigan), USA.
[24] Cox, T.F., Cox, MAA. (2000) Multidimensional Scaling, 2nd ed. Chapman and Hall/CRC.
[25] Borg, I., Groenen, PJF. (2005) Modern multidimensional scaling. 2nd ed. New York: Springer.
[26] Helliwel, P. S., Evans, P. F., Wright, V. (1994) The Straight cervical spine: does it indicate muscle spasm? *J Bone Joint Surg*, **76-B**(1): pp.103–6.
[27] Haedacker, J. W., Shuford, R. F., Capicoto, P. N., Pryor, P. W. (1997) Radiographic standing cervical segmental alignment in adult volunteers without neck symptoms. *Spine*, **22**(13): pp.1472–80.
[28] Klinich, K.D., Ebert, S.M. *et al*., (2004) Cervical spine geometry in the automotive seated posture: variations with age, stature, and gender. *Stapp Car Crash Journal*, **48**: pp. 301-330.
[29] Klinich, K.D., Ebert, S.M., Reed, M.P. (2012). Quantifying cervical spine curvature using Bézier splines. *Journal of Biomechanical Engineering*, **11**(4): 114503-114508.
[30] Newell, R. S., Siegmund, G. P., Blouin, J. S., Street, J., Cripton, P. A. (2014) Cervical vertebral realignment when voluntarily adopting a protective neck posture. *Spine*, **39**(15): pp.E885-93.
[31] Lee, J. H., Park, Y. K., Kim, J. H. (2014) Chronic neck pain in young adults: perspectives on anatomic differences. *Spine J*, **14**: pp.2628–38.
[32] Park, S. M., Song, K. S., Park, S. H., Kang, H., Riew, K. D. (2015) Does whole-spine lateral radiograph with clavicle positioning reflect the correct cervical sagittal alignments? *Eur Spine J*, **24**: pp.57–62.
[33] Endo, K., Suzuki, H. *et al*. (2014) Characteristics of Sagittal Spino-Pelvic Alignment in Japanese Young Adults. *Asian Spine J*, **8**(5): pp.599–604.

VIII. APPENDIX

In this section, normalised whole spine alignments are provided in their original position. The sacrum is at the origin, and the length between C2 and the sacrum is 1 in each figure.

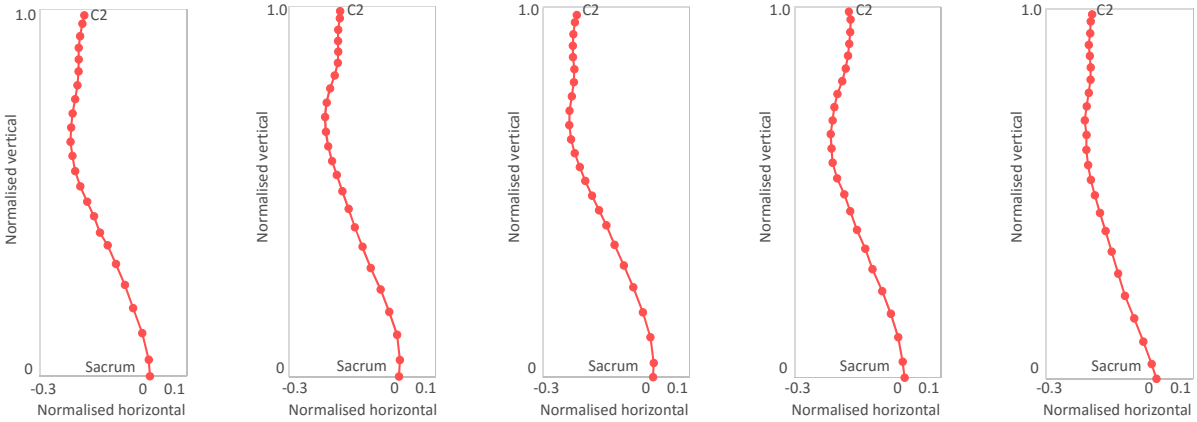

(a) F-J-1 (b) F-J-2 (c) F-J-3 (d) F-J-4 (e) F-J-5

Fig. A-1 Whole spine alignments of Japanese female subjects. The Caption of each figure indicates a corresponding subject ID in Table I.

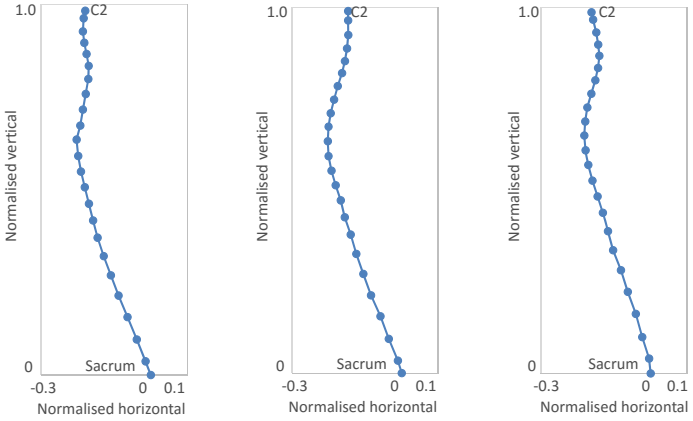

(a) M-J-1 (b) M-J-2 (c) M-J-3

Fig. A-2 Whole spine alignments of Japanese male subjects. The Caption of each figure indicates a corresponding subject ID in Table I.

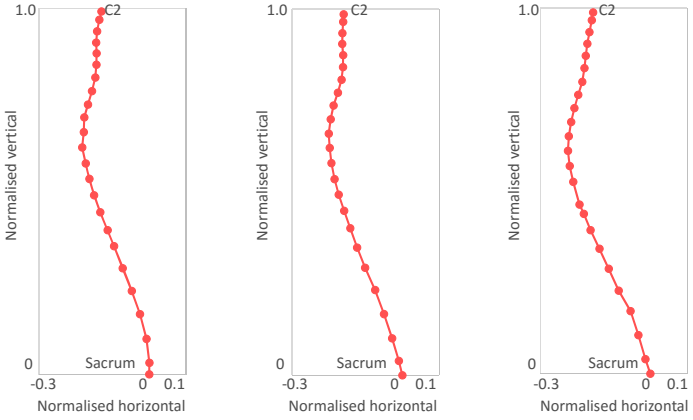

(a) F-E-1 (b) F-E-2 (c) F-E-3

Fig. A-3 Whole spine alignments of European female subjects. The Caption of each figure indicates a corresponding subject ID in Table II.

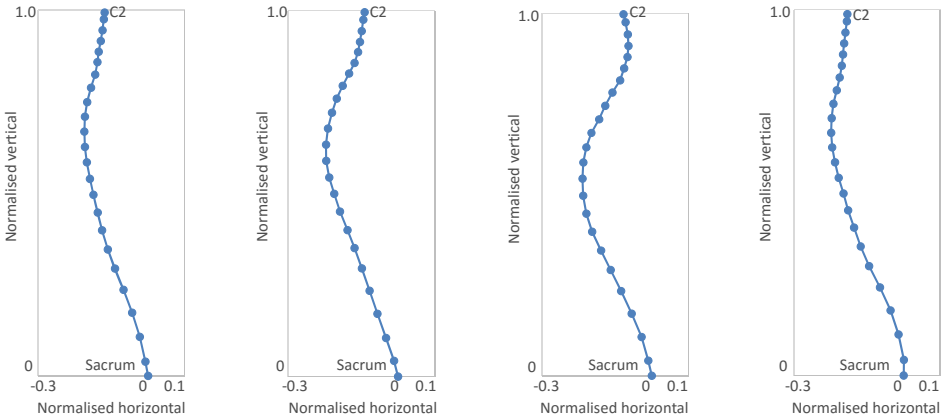

(a) M-E-1 (b) M-E-2 (c) M-E-3 (d) M-E-4

Fig. A-4 Whole spine alignments of European male subjects. The Caption of each figure indicates a corresponding subject ID in Table II.

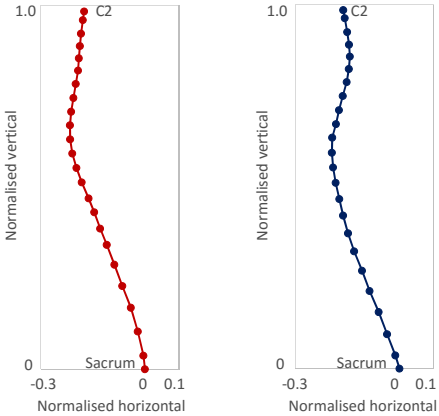

(a) Female (b) Male

Fig. A-5 The estimated Whole spine alignments for female and male subjects. Fig. A-5 (a) and (b) were obtained by rotating back whole spine alignments shown in Fig. 13(b) to their original positions.

Table A-I
Normalised coordinate data at each vertebra for Japanese female subjects

	F-J-1		F-J-2		F-J-3		F-J-4		F-J-5	
	Horizontal	Vertical	Horizontal	Vertical	Horizontal	Vertical	Horizontal	Vertical	Horizontal	Vertical
C2	-0.179	0.984	-0.161	0.987	-0.208	0.978	-0.152	0.988	-0.176	0.984
C3	-0.184	0.961	-0.162	0.968	-0.213	0.959	-0.148	0.967	-0.180	0.965
C4	-0.190	0.927	-0.166	0.937	-0.218	0.927	-0.148	0.933	-0.181	0.933
C5	-0.194	0.896	-0.166	0.906	-0.219	0.896	-0.151	0.902	-0.185	0.902
C6	-0.194	0.864	-0.166	0.877	-0.219	0.865	-0.155	0.869	-0.182	0.872
C7	-0.194	0.831	-0.167	0.847	-0.215	0.832	-0.161	0.835	-0.179	0.841
T1	-0.197	0.793	-0.176	0.813	-0.216	0.797	-0.170	0.801	-0.180	0.808
T2	-0.203	0.755	-0.188	0.778	-0.222	0.759	-0.183	0.766	-0.185	0.772
T3	-0.210	0.716	-0.198	0.740	-0.228	0.720	-0.192	0.731	-0.190	0.736
T4	-0.214	0.678	-0.202	0.701	-0.229	0.681	-0.197	0.695	-0.196	0.698
T5	-0.216	0.639	-0.200	0.661	-0.224	0.643	-0.202	0.658	-0.191	0.659
T6	-0.211	0.601	-0.193	0.622	-0.214	0.605	-0.199	0.619	-0.191	0.619
T7	-0.203	0.559	-0.183	0.582	-0.200	0.568	-0.197	0.580	-0.186	0.577
T8	-0.190	0.518	-0.170	0.545	-0.185	0.530	-0.184	0.538	-0.179	0.537
T9	-0.171	0.476	-0.155	0.500	-0.167	0.490	-0.165	0.495	-0.168	0.495
T10	-0.152	0.436	-0.138	0.453	-0.147	0.451	-0.149	0.449	-0.154	0.448
T11	-0.136	0.392	-0.121	0.403	-0.127	0.410	-0.130	0.399	-0.139	0.399
T12	-0.115	0.357	-0.100	0.351	-0.105	0.357	-0.107	0.348	-0.122	0.343
L1	-0.093	0.306	-0.077	0.293	-0.080	0.301	-0.088	0.293	-0.104	0.284
L2	-0.069	0.249	-0.050	0.235	-0.054	0.243	-0.061	0.233	-0.086	0.224
L3	-0.046	0.186	-0.027	0.175	-0.028	0.175	-0.038	0.173	-0.061	0.163
L4	-0.021	0.117	-0.005	0.113	-0.007	0.108	-0.018	0.109	-0.036	0.100
L5	-0.003	0.045	0.002	0.044	0.002	0.038	-0.006	0.043	-0.013	0.040
S	0.000	0.000	0.000	0.000	0.000	0.000	0.000	0.000	0.000	0.000

Table A-II
Normalised coordinate data at each vertebra for Japanese male subjects

	M-J-1		M-J-2		M-J-3	
	Horizontal	Vertical	Horizontal	Vertical	Horizontal	Vertical
C2	-0.179	0.984	-0.147	0.989	-0.161	0.987
C3	-0.183	0.963	-0.146	0.964	-0.157	0.967
C4	-0.185	0.928	-0.146	0.924	-0.149	0.932
C5	-0.182	0.897	-0.149	0.887	-0.143	0.899
C6	-0.175	0.867	-0.155	0.853	-0.140	0.868
C7	-0.169	0.835	-0.163	0.820	-0.144	0.835
T1	-0.170	0.800	-0.175	0.785	-0.151	0.801
T2	-0.178	0.759	-0.185	0.747	-0.162	0.764
T3	-0.185	0.717	-0.194	0.710	-0.173	0.727
T4	-0.192	0.674	-0.200	0.674	-0.178	0.689
T5	-0.202	0.635	-0.202	0.634	-0.181	0.650
T6	-0.198	0.592	-0.200	0.593	-0.178	0.610
T7	-0.191	0.549	-0.192	0.553	-0.170	0.570
T8	-0.180	0.507	-0.181	0.513	-0.159	0.527
T9	-0.169	0.462	-0.166	0.472	-0.145	0.484
T10	-0.157	0.417	-0.155	0.426	-0.130	0.439
T11	-0.145	0.371	-0.140	0.378	-0.117	0.388
T12	-0.129	0.321	-0.124	0.326	-0.103	0.337
L1	-0.109	0.269	-0.105	0.271	-0.081	0.282
L2	-0.088	0.214	-0.084	0.212	-0.063	0.223
L3	-0.064	0.156	-0.058	0.155	-0.041	0.163
L4	-0.038	0.096	-0.036	0.094	-0.023	0.099
L5	-0.014	0.037	-0.011	0.034	-0.004	0.041
S	0.000	0.000	0.000	0.000	0.000	0.000

Table A-III
Normalised coordinate data at each vertebra for European female subjects

	F-E-1		F-E-2		F-E-3	
	Horizontal	Vertical	Horizontal	Vertical	Horizontal	Vertical
C2	-0.130	0.991	-0.160	0.987	-0.156	0.988
C3	-0.136	0.969	-0.162	0.967	-0.160	0.966
C4	-0.142	0.937	-0.164	0.935	-0.166	0.934
C5	-0.145	0.907	-0.164	0.906	-0.172	0.902
C6	-0.144	0.877	-0.162	0.875	-0.176	0.869
C7	-0.144	0.846	-0.162	0.843	-0.180	0.835
T1	-0.147	0.811	-0.166	0.808	-0.186	0.798
T2	-0.156	0.774	-0.176	0.773	-0.197	0.763
T3	-0.167	0.737	-0.188	0.738	-0.207	0.726
T4	-0.177	0.702	-0.196	0.700	-0.216	0.688
T5	-0.179	0.662	-0.201	0.661	-0.222	0.649
T6	-0.183	0.620	-0.199	0.622	-0.225	0.609
T7	-0.173	0.576	-0.194	0.580	-0.220	0.568
T8	-0.163	0.534	-0.185	0.537	-0.210	0.525
T9	-0.150	0.489	-0.174	0.494	-0.193	0.462
T10	-0.134	0.443	-0.159	0.450	-0.181	0.437
T11	-0.114	0.394	-0.142	0.402	-0.163	0.392
T12	-0.096	0.350	-0.124	0.349	-0.139	0.342
L1	-0.073	0.290	-0.102	0.294	-0.114	0.287
L2	-0.048	0.228	-0.075	0.233	-0.086	0.227
L3	-0.025	0.164	-0.050	0.168	-0.054	0.171
L4	-0.008	0.097	-0.028	0.101	-0.033	0.105
L5	0.000	0.032	-0.009	0.039	-0.014	0.040
S	0.000	0.000	0.000	0.000	0.000	0.000

Table A-IV
Normalised coordinate data at each vertebra for European male subjects

	M-E-1		M-E-2		M-E-3		M-E-4	
	Horizontal	Vertical	Horizontal	Vertical	Horizontal	Vertical	Horizontal	Vertical
C2	-0.118	0.993	-0.091	0.996	-0.077	0.997	-0.154	0.988
C3	-0.121	0.975	-0.095	0.975	-0.072	0.975	-0.155	0.969
C4	-0.124	0.945	-0.100	0.944	-0.066	0.942	-0.159	0.938
C5	-0.129	0.915	-0.104	0.915	-0.064	0.910	-0.163	0.908
C6	-0.135	0.886	-0.109	0.887	-0.067	0.879	-0.166	0.878
C7	-0.138	0.858	-0.119	0.857	-0.075	0.848	-0.169	0.847
T1	-0.144	0.823	-0.134	0.828	-0.086	0.815	-0.175	0.815
T2	-0.156	0.788	-0.151	0.795	-0.107	0.781	-0.183	0.780
T3	-0.166	0.748	-0.167	0.759	-0.127	0.745	-0.192	0.743
T4	-0.172	0.708	-0.180	0.721	-0.144	0.708	-0.197	0.703
T5	-0.174	0.668	-0.191	0.678	-0.165	0.670	-0.198	0.664
T6	-0.172	0.626	-0.197	0.634	-0.179	0.630	-0.195	0.624
T7	-0.167	0.584	-0.196	0.590	-0.187	0.588	-0.188	0.583
T8	-0.159	0.538	-0.188	0.544	-0.189	0.544	-0.177	0.540
T9	-0.149	0.495	-0.174	0.499	-0.187	0.497	-0.164	0.498
T10	-0.137	0.446	-0.158	0.451	-0.178	0.447	-0.152	0.452
T11	-0.125	0.398	-0.138	0.400	-0.163	0.397	-0.136	0.404
T12	-0.110	0.345	-0.119	0.351	-0.139	0.345	-0.117	0.353
L1	-0.090	0.293	-0.099	0.296	-0.112	0.292	-0.094	0.299
L2	-0.067	0.235	-0.078	0.235	-0.084	0.234	-0.065	0.241
L3	-0.044	0.173	-0.056	0.172	-0.055	0.171	-0.036	0.178
L4	-0.023	0.106	-0.033	0.105	-0.028	0.107	-0.014	0.112
L5	-0.007	0.039	-0.011	0.043	-0.010	0.041	0.000	0.042
S	0.000	0.000	0.000	0.000	0.000	0.000	0.000	0.000

Table A-V
Normalised coordinate data at each vertebra for the estimated average spinal alignments

	Female		Male	
	Horizontal	Vertical	Horizontal	Vertical
C2	-0.175	0.985	-0.162	0.987
C3	-0.179	0.961	-0.158	0.964
C4	-0.184	0.924	-0.151	0.926
C5	-0.188	0.889	-0.146	0.891
C6	-0.191	0.856	-0.143	0.858
C7	-0.193	0.822	-0.146	0.824
T1	-0.199	0.785	-0.152	0.788
T2	-0.206	0.747	-0.164	0.750
T3	-0.213	0.709	-0.175	0.711
T4	-0.216	0.672	-0.184	0.673
T5	-0.216	0.633	-0.194	0.635
T6	-0.209	0.593	-0.196	0.594
T7	-0.198	0.554	-0.192	0.554
T8	-0.182	0.515	-0.184	0.511
T9	-0.162	0.470	-0.174	0.467
T10	-0.146	0.432	-0.163	0.421
T11	-0.129	0.387	-0.149	0.373
T12	-0.110	0.342	-0.131	0.323
L1	-0.088	0.288	-0.108	0.270
L2	-0.065	0.229	-0.086	0.213
L3	-0.041	0.169	-0.060	0.156
L4	-0.020	0.104	-0.036	0.095
L5	-0.004	0.037	-0.012	0.036
S	0.000	0.000	0.000	0.000

Table A-VI
Length between C2 and the sacrum of the original data set for Japanese female subjects

	F-J-1	F-J-2	F-J-3	F-J-4	F-J-5
C2-S length [mm]	465	524	509	504	530

Table A-VII
Length between C2 and the sacrum of the original data set for Japanese male subjects

	M-J-1	M-J-2	M-J-3
C2-S length [mm]	534	575	538

Table A-VIII
Length between C2 and the sacrum of the original data set for European female subjects

	F-E-1	F-E-2	F-E-3
C2-S length [mm]	498	528	490

Table A-IX
Length between C2 and the sacrum of the original data set for European male subjects

	M-E-1	M-E-2	M-E-3	F-E-4
C2-S length [mm]	547	539	521	553